Ballistic photocurrents in semiconductor quantum wells caused by the excitation of asymmetric excitons

Huynh Thanh Duc,[1,2] Cong Ngo,[1] and Torsten Meier[3]
[1]*Ho Chi Minh City Institute of Physics, Vietnam Academy of Science and Technology, 1 Mac Dinh Chi, District 1, Ho Chi Minh City 70072, Vietnam*
[2]*Graduate University of Science and Technology, Vietnam Academy of Science and Technology, 18 Hoang Quoc Viet, Hanoi 10072, Vietnam*
[3]*Department of Physics and CeOPP, Universität Paderborn, Warburger Strasse 100, D-33098 Paderborn, Germany*

(Received 11 May 2019; published 22 July 2019)

We theoretically investigate the generation and dynamics of photocurrents induced by linearly polarized single-frequency light pulses in GaAs quantum wells. Our approach is based on the multiband semiconductor Bloch equations (SBE) formulated in the basis of eigenfunctions on the 14-band $\mathbf{k}\cdot\mathbf{p}$ model and includes excitonic effects and carrier longitudinal-optical-phonon scattering processes. By solving the SBE, we obtain both shift and ballistic currents. For a particular excitation geometry, we obtain a ballistic current which is absent if the electron-hole attraction is neglected. Whereas in other cases excitonic effects quantitatively modify photocurrents that originate from single-particle properties, here we demonstrate the existence of a ballistic current which is absent in single-particle calculations. This photocurrent is of second order in the light-matter interaction and is purely caused by the asymmetric electron-hole Coulomb attraction that results from the inversion asymmetry of GaAs. Furthermore, we show that the coherent dynamics of excitonic wave packets gives rise to oscillations in the photocurrent transients.

DOI: 10.1103/PhysRevB.100.045308

I. INTRODUCTION

The inversion asymmetry of the crystal structure of many semiconductors allows for the appearance of photocurrents which are of second order in the light-matter interaction. One distinguishes three different contributions to the photocurrents. The first term, called ballistic or injection current, originates from an asymmetry in the momentum distribution of photoexcited carriers. Ballistic currents can be generated by optical excitation with circularly polarized light and therefore they are referred to as a circular photovoltaic (or photogalvanic) effect [1–3]. For the case of excitation with linear polarized light, some additional processes, such as asymmetric electron-hole and electron-phonon scatterings, are required for the generation of ballistic currents [2,4]. The second term results from shifts of electrons in real space when they are photoexcited from the valence to the conduction band, and hence this term is called the shift current [2,3,5]. The third term, named rectification current, arises due to the dynamics of nonresonant polarizations. Unlike ballistic and shift currents which require a resonant excitation, a rectification current exists for all photon energies since all nonresonant polarizations can make a contribution [3,6,7].

The generation of ultrafast coherent photocurrents by excitation with single-frequency light in noncentrosymmetric semiconductor systems has received considerable attention [1–26]. Perturbation theory for the light-matter interaction has been widely used in previous theoretical approaches [3,4,7,9,10,12]. To the best of our knowledge, Shelest and Éntin were the first to describe the contribution of excitonic effects to the photovoltaic effect [4]. Their approach is based on perturbative calculations using Fermi's golden rule. By evaluating Fermi's golden rule with unbound solutions of the Wannier equation for excitons as the final states, they obtained the optical transition rate with electron-hole attraction. In noncentrosymmetric crystals, the asymmetric electron-hole attraction can result in different transition rates at momenta $\pm\mathbf{k}$ and, therefore, lead to a ballistic current. Though this current has been known for a long time, its temporal evolution which requires the evaluation of dynamic equations has rarely been investigated. Recently, microscopic and nonperturbative calculations for shift currents including excitonic effects in bulk semiconductors have been performed [24]. However, ballistic currents were not considered in these calculations.

In this work, we employ the microscopic approach developed in Refs. [17,23] to analyze the coherent dynamics of photocurrents induced by linearly polarized single-frequency laser pulses in GaAs quantum wells (QWs). By including the electron-hole interaction, we also obtain, besides shift currents, ballistic currents which are caused by the asymmetric electron-hole attraction. The formation of bound excitons leads to several interesting effects which we analyze below. If the incident light pulse has a sufficiently large spectral width, it can simultaneously excite multiple exciton states with different energies. The interference between these excitonic coherences results in coherent excitonic beats. This phenomenon has been observed by four-wave mixing experiments [27–29] and here we show that the dynamics of excitonic wave packets also leads to oscillations of the ballistic current transients. We furthermore analyze the decay of photocurrents. We restrict ourselves to the low-density limit in which carrier-carrier scattering processes can be neglected and the carrier-phonon scattering dominates the relaxation and

dephasing dynamics of photoexcited semiconductors. The carrier longitudinal-optical (LO)-phonon interaction is included in our approach on the level of a second-order Born-Markov approximation.

This paper is organized as follows. In Sec. II, we describe our theoretical approach, i.e., the derivation of the semiconductor Bloch equations (SBE) in the basis of eigenfunctions of the 14-band $\mathbf{k}\cdot\mathbf{p}$ band structure model, which includes the electron-hole attraction effects and carrier-LO phonon scattering processes. Numerical results are presented and discussed in Sec. III. Our main results are briefly summarized in Sec. IV.

II. THEORETICAL APPROACH

In the framework of the envelope function approximation, the wave function of an electron in a semiconductor QW grown along the z axis is written as

$$\psi^{\lambda}_{\mathbf{k}_\parallel}(\mathbf{r}) = \frac{1}{\sqrt{L^3}} e^{i\mathbf{k}_\parallel\cdot\mathbf{r}_\parallel} u^{\lambda}_{\mathbf{k}_\parallel}(\mathbf{r}),\quad u^{\lambda}_{\mathbf{k}_\parallel}(\mathbf{r}) = \sum_{n=1}^{14} f^{\lambda}_{n\mathbf{k}_\parallel}(z) u_n(\mathbf{r}), \tag{1}$$

where λ denotes the band index, $\mathbf{k}_\parallel = (k_x, k_y)$ is the in-plane wave vector, and $u_n(\mathbf{r})$ are the basis functions of the 14-band $\mathbf{k}\cdot\mathbf{p}$ model. $f^{\lambda}_{n\mathbf{k}_\parallel}(z)$ are slowly varying envelope functions which satisfy the equation

$$\sum_{m=1}^{14}\left[H^{\mathbf{k}\cdot\mathbf{p}}_{nm}\left(\mathbf{k}_\parallel, -i\frac{\partial}{\partial z}\right) + V^{\mathrm{conf}}_n(z)\delta_{nm}\right] f^{\lambda}_{m\mathbf{k}_\parallel}(z) = \varepsilon^{\lambda}_{\mathbf{k}_\parallel} f^{\lambda}_{n\mathbf{k}_\parallel}(z). \tag{2}$$

Here, $H^{\mathbf{k}\cdot\mathbf{p}}(\mathbf{k})$ is the 14-band $\mathbf{k}\cdot\mathbf{p}$ Hamiltonian, $V^{\mathrm{conf}}(z)$ is the band-offset potential of the well, and $\varepsilon^{\lambda}_{\mathbf{k}_\parallel}$ is the band energy. The 14-band $\mathbf{k}\cdot\mathbf{p}$ model includes the spin-orbit interaction as well as the inversion asymmetry of the involved materials [17,23,30].

We now simplify the notation using $\mathbf{k}$ instead of $\mathbf{k}_\parallel$. In the single-particle basis consisting of the Bloch states $\psi^{\lambda}_{\mathbf{k}}(\mathbf{r})$, we write the many-body Hamiltonian for the photoexcited semiconductor QW system as [17]

$$\begin{aligned} H = &\sum_{\lambda,\mathbf{k}} \varepsilon^{\lambda}_{\mathbf{k}} a^{+}_{\lambda\mathbf{k}} a_{\lambda\mathbf{k}} + \frac{1}{2}\sum_{\lambda_1,\lambda_2,\lambda_3,\lambda_4,\mathbf{k},\mathbf{k}',\mathbf{k}''} V^{\lambda_1\lambda_2\lambda_3\lambda_4}_{\mathbf{k},\mathbf{k}',\mathbf{k}''} a^{+}_{\lambda_1\mathbf{k}+\mathbf{k}''} a^{+}_{\lambda_2\mathbf{k}'-\mathbf{k}''} a_{\lambda_3\mathbf{k}'} a_{\lambda_4\mathbf{k}} + \sum_{\mathbf{q}} \hbar\omega_{\mathbf{q}}(b^{+}_{\mathbf{q}} b_{\mathbf{q}} + 1/2) \\ &+ \sum_{\lambda,\lambda',\mathbf{k},\mathbf{q}} g^{\lambda\lambda'}_{\mathbf{k}+\mathbf{q},\mathbf{k}} a^{+}_{\lambda\mathbf{k}+\mathbf{q}} a_{\lambda'\mathbf{k}}(b_{\mathbf{q}} + b^{+}_{-\mathbf{q}}) + e\mathbf{A}(t)\sum_{\lambda,\lambda',\mathbf{k}} \mathbf{v}^{\lambda\lambda'}_{\mathbf{k}} a^{+}_{\lambda\mathbf{k}} a_{\lambda'\mathbf{k}}, \end{aligned} \tag{3}$$

where $a^{+}_{\lambda\mathbf{k}}$ ($a_{\lambda\mathbf{k}}$) is the creation (annihilation) operator of an electron at wave vector $\mathbf{k}$ in band λ and $b^{+}_{\mathbf{q}}$ ($b_{\mathbf{q}}$) is the creation (annihilation) operator of a phonon with wave vector $\mathbf{q}$ and energy $\hbar\omega_{\mathbf{q}}$.

The Coulomb matrix element is given by

$$V^{\lambda_1\lambda_2\lambda_3\lambda_4}_{\mathbf{k},\mathbf{k}',\mathbf{k}''} = V_{\mathbf{k}''}\kappa^{\lambda_1\lambda_2\lambda_3\lambda_4}_{\mathbf{k},\mathbf{k}',\mathbf{k}''}, \tag{4}$$

where $V_{\mathbf{k}} = \frac{2\pi e^2}{\epsilon_\infty L^2}\frac{1}{|\mathbf{k}|}$ is the ideal two-dimensional Coulomb potential, and the factor

$$\kappa^{\lambda_1\lambda_2\lambda_3\lambda_4}_{\mathbf{k},\mathbf{k}',\mathbf{k}''} = \int dz \int dz'\, e^{-|\mathbf{k}''||z'-z|} \times \sum_{n=1}^{14} f^{\lambda_1 *}_{n\mathbf{k}+\mathbf{k}''}(z) f^{\lambda_4}_{n\mathbf{k}}(z) \sum_{n=1}^{14} f^{\lambda_2 *}_{n\mathbf{k}'-\mathbf{k}''}(z') f^{\lambda_3}_{n\mathbf{k}'}(z') \tag{5}$$

contains the envelope functions and thus the structural characteristics of the material. It is important to note that in noncentrosymmetric media, κ is not invariant under spatial inversion, i.e., $\kappa^{\lambda_1\lambda_2\lambda_3\lambda_4}_{\mathbf{k},\mathbf{k}',\mathbf{k}''} \neq \kappa^{\lambda_1\lambda_2\lambda_3\lambda_4}_{-\mathbf{k},-\mathbf{k}',-\mathbf{k}''}$. As is shown below, this missing symmetry is responsible for the appearance of ballistic currents when excitonic resonances are excited. Since the $\mathbf{k}$-space Coulomb matrix element is asymmetric, we will refer to the bound excitonic states as asymmetric excitons.

The matrix element that determines the coupling of electrons to dispersionless LO phonon is written as [10,31]

$$g^{\lambda\lambda'}_{\mathbf{k}+\mathbf{q},\mathbf{k}} = g_{\mathbf{q}}\gamma^{\lambda\lambda'}_{\mathbf{k}+\mathbf{q},\mathbf{k}}, \tag{6}$$

where $g_{\mathbf{q}}$ is defined by the Fröhlich relation,

$$g^2_{\mathbf{q}} = \frac{1}{2}\hbar\omega_{\mathrm{LO}} V_{\mathbf{q}}\left(1 - \frac{\epsilon_\infty}{\epsilon_0}\right), \tag{7}$$

and the structure factor $\gamma^{\lambda\lambda'}_{\mathbf{k}+\mathbf{q},\mathbf{k}}$ reads

$$\gamma^{\lambda\lambda'}_{\mathbf{k}+\mathbf{q},\mathbf{k}} = \int dz \sum_n f^{\lambda *}_{n\mathbf{k}+\mathbf{q}}(z) f^{\lambda'}_{n\mathbf{k}}(z). \tag{8}$$

For GaAs, we use $\hbar\omega_{\mathrm{LO}} = 36$ meV, $\epsilon_0 = 12.9$, and $\epsilon_\infty = 10.9$.

The light-matter interaction is described in the velocity gauge which contains the vector potential $\mathbf{A}(t)$ of the light field and the electron velocity matrix element,

$$\mathbf{v}^{\lambda\lambda'}_{\mathbf{k}} = \int dz \sum_{n,m=1}^{14} f^{\lambda *}_{n\mathbf{k}}(z)\left(\frac{1}{\hbar}\nabla_{\mathbf{k}} H^{\mathbf{k}\cdot\mathbf{p}}\right)_{nm} f^{\lambda'}_{m\mathbf{k}}(z). \tag{9}$$

The relation between the vector potential $\mathbf{A}(t)$ and the electric field $\mathbf{E}(t)$ of the exciting light is given by $\mathbf{A}(t) = \int_{-\infty}^{t} dt'\mathbf{E}(t')$. The electric field of a linearly polarized Gaussian light pulse that propagates in the z direction is described by

$$\mathbf{E}(t) = E_0(\cos\theta, \sin\theta, 0) e^{-t^2/2\tau_L^2} e^{i\omega t} + \mathrm{c.c.}, \tag{10}$$

where E_0 is the maximal amplitude, θ is the polarization angle with respect to the x axis, τ_L is the duration of the Gaussian envelope, and ω is the central frequency.

Evaluating the Heisenberg equations of motion for expectation values $x^{\lambda\lambda'}_{\mathbf{k}} = \langle a^{+}_{\lambda\mathbf{k}} a_{\lambda'\mathbf{k}}\rangle$ and treating the many-body Coulomb interaction in the time-dependent Hartree-Fock approximation, we obtain the SBE as [17,32]

$$\frac{d}{dt}x^{\lambda\lambda'}_{\mathbf{k}} = \frac{i}{\hbar}\left(\varepsilon^{\lambda}_{\mathbf{k}} - \varepsilon^{\lambda'}_{\mathbf{k}}\right)x^{\lambda\lambda'}_{\mathbf{k}} + i\sum_{\mu}\left(\Omega^{\mu\lambda}_{\mathbf{k}} x^{\mu\lambda'}_{\mathbf{k}} - \Omega^{\lambda'\mu}_{\mathbf{k}} x^{\lambda\mu}_{\mathbf{k}}\right) + \left.\frac{d}{dt}x^{\lambda\lambda'}_{\mathbf{k}}\right|_{\mathrm{scatt}}, \tag{11}$$

with

$$\Omega_{\mathbf{k}}^{\mu\mu'} = \frac{1}{\hbar}\left[e\mathbf{A}(t)\cdot\mathbf{v}_{\mathbf{k}}^{\mu\mu'} - \sum_{\nu,\nu',\mathbf{k}'} V_{\mathbf{k},\mathbf{k}'}^{\nu\mu\nu'\mu'} x_{\mathbf{k}'}^{\nu\nu'}\right]. \tag{12}$$

Here, $x_{\mathbf{k}}^{\lambda\lambda'}$ represents either an occupation ($\lambda = \lambda'$) or a coherence between two different bands or subbands ($\lambda \neq \lambda'$) and we have introduced the notation $V_{\mathbf{k},\mathbf{k}'}^{\nu\mu\nu'\mu'}$ instead of $V_{\mathbf{k},\mathbf{k}',\mathbf{k}'-\mathbf{k}}^{\nu\mu\nu'\mu'}$ for the Coulomb matrix elements. The term denoted by $|_{\text{scatt}}$ refers to scattering processes. In the low-density limit, the carrier-carrier scattering rate is small and therefore neglected. Here we treat the electron LO-phonon interaction on the second Born-Markov level, which results in the following scattering contributions for the occupations:

$$\begin{aligned}\left.\frac{d}{dt}x_{\mathbf{k}}^{\lambda\lambda}\right|_{\text{scatt}} \simeq \frac{2\pi}{\hbar^2}\sum_{\mu,\mathbf{q}}\Bigg\{&\delta\left(\frac{\varepsilon_{\mathbf{k}+\mathbf{q}}^{\mu}}{\hbar} - \frac{\varepsilon_{\mathbf{k}}^{\lambda}}{\hbar} - \omega_{\mathbf{q}}\right)\left|g_{\mathbf{k}+\mathbf{q},\mathbf{k}}^{\mu\lambda}\right|^2\left[x_{\mathbf{k}+\mathbf{q}}^{\mu\mu}\left(1-x_{\mathbf{k}}^{\lambda\lambda}\right)(N_{\mathbf{q}}+1) - x_{\mathbf{k}}^{\lambda\lambda}\left(1-x_{\mathbf{k}+\mathbf{q}}^{\mu\mu}\right)N_{\mathbf{q}}\right]\\ &-\delta\left(\frac{\varepsilon_{\mathbf{k}+\mathbf{q}}^{\mu}}{\hbar} - \frac{\varepsilon_{\mathbf{k}}^{\lambda}}{\hbar} + \omega_{\mathbf{q}}\right)\left|g_{\mathbf{k}+\mathbf{q},\mathbf{k}}^{\mu\lambda}\right|^2\left[x_{\mathbf{k}}^{\lambda\lambda}\left(1-x_{\mathbf{k}+\mathbf{q}}^{\mu\mu}\right)(N_{\mathbf{q}}+1) - x_{\mathbf{k}+\mathbf{q}}^{\mu\mu}\left(1-x_{\mathbf{k}}^{\lambda\lambda}\right)N_{\mathbf{q}}\right]\Bigg\},\end{aligned} \tag{13}$$

and for the coherences ($\lambda \neq \lambda'$),

$$\begin{aligned}\left.\frac{d}{dt}x_{\mathbf{k}}^{\lambda\lambda'}\right|_{\text{scatt}} \simeq -\frac{x_{\mathbf{k}}^{\lambda\lambda'}}{\hbar^2}\sum_{\mu,\mathbf{q}}\Bigg\{&\left[\mathcal{D}\left(\frac{\varepsilon_{\mathbf{k}+\mathbf{q}}^{\mu}}{\hbar} - \frac{\varepsilon_{\mathbf{k}}^{\lambda'}}{\hbar} - \omega_{\mathbf{q}}\right)\left|g_{\mathbf{k}+\mathbf{q},\mathbf{k}}^{\mu\lambda}\right|^2 + \mathcal{D}\left(\frac{\varepsilon_{\mathbf{k}}^{\lambda}}{\hbar} - \frac{\varepsilon_{\mathbf{k}+\mathbf{q}}^{\mu}}{\hbar} + \omega_{\mathbf{q}}\right)\left|g_{\mathbf{k},\mathbf{k}+\mathbf{q}}^{\lambda'\mu}\right|^2\right]\left(N_{\mathbf{q}} + x_{\mathbf{k}+\mathbf{q}}^{\mu\mu}\right)\\ &+\left[\mathcal{D}\left(\frac{\varepsilon_{\mathbf{k}+\mathbf{q}}^{\mu}}{\hbar} - \frac{\varepsilon_{\mathbf{k}}^{\lambda'}}{\hbar} + \omega_{\mathbf{q}}\right)\left|g_{\mathbf{k}+\mathbf{q},\mathbf{k}}^{\mu\lambda}\right|^2 + \mathcal{D}\left(\frac{\varepsilon_{\mathbf{k}}^{\lambda}}{\hbar} - \frac{\varepsilon_{\mathbf{k}+\mathbf{q}}^{\mu}}{\hbar} - \omega_{\mathbf{q}}\right)\left|g_{\mathbf{k},\mathbf{k}+\mathbf{q}}^{\lambda'\mu}\right|^2\right]\left(N_{\mathbf{q}} + 1 - x_{\mathbf{k}+\mathbf{q}}^{\mu\mu}\right)\Bigg\},\end{aligned} \tag{14}$$

where $\mathcal{D}(\omega) = \int_0^\infty dt\, e^{i\omega t}$ and $N_{\mathbf{q}} = [\exp(\hbar\omega_{\text{LO}}/k_BT) - 1]^{-1}$ is the Bose-Einstein distribution.

The huge number of Coulomb matrix elements that appear when implementing Eq. (12) numerically is a challenge for the numerical evaluation. We therefore focus on the most important ones and take into account the Coulomb matrix elements $V_{\mathbf{k},\mathbf{k}'}^{vcc'v'}$ and $V_{\mathbf{k},\mathbf{k}'}^{cvv'c'}$, where c, c' (v, v') are conduction- (valence)-band indices, i.e., the matrix elements describing the electron-hole attraction which give rise to excitonic effects. The Coulomb interaction between electrons in the conduction and in the valence bands and also Auger terms, which induce interband transitions, are not expected to influence our results significantly and are neglected.

The dynamics of the photoexcited semiconductor system is obtained by solving the SBE (11). From the solutions of the SBE, we compute the density of the charge current induced by the optical excitation via

$$\mathbf{j}(t) = \frac{e}{L^2}\sum_{\lambda,\lambda',\mathbf{k}} \mathbf{v}_{\mathbf{k}}^{\lambda\lambda'} x_{\mathbf{k}}^{\lambda\lambda'}(t). \tag{15}$$

The total current $\mathbf{j}$ can be separated into a diagonal contribution,

$$\mathbf{j}_{\text{ball}}(t) = \frac{e}{L^2}\sum_{\lambda,\mathbf{k}} \mathbf{v}_{\mathbf{k}}^{\lambda\lambda} x_{\mathbf{k}}^{\lambda\lambda}(t), \tag{16}$$

describing the ballistic current and an off-diagonal contribution,

$$\mathbf{j}_{\text{od}}(t) = \frac{e}{L^2}\sum_{\lambda,\lambda\neq\lambda',\mathbf{k}} \mathbf{v}_{\mathbf{k}}^{\lambda\lambda'} x_{\mathbf{k}}^{\lambda\lambda'}(t). \tag{17}$$

As in Refs. [23,24], we use a filter in frequency space to separate out the low-frequency parts of $\mathbf{j}_{\text{od}}(\omega)$ and an inverse Fourier transformation to obtain the shift current $\mathbf{j}_{\text{shift}}(t)$.

III. NUMERICAL RESULTS AND DISCUSSION

We consider a GaAs/$Al_{0.35}Ga_{0.65}$As QW of 8 nm thickness grown along the [110] crystallographic direction. The QW system is presented in the coordinate system (x, y, z) with $x \parallel [001]$, $y \parallel [1\bar{1}0]$, and $z \parallel [110]$. The band structure of the QW is obtained from the solution of Eq. (2) using $\mathbf{k}\cdot\mathbf{p}$ parameters for GaAs and AlGaAs taken from Ref. [30]. The temperature dependence of the band gap is described by the Varshni relation. Our calculations are performed for the temperature of $T = 300$ K. In our solutions of the multiband SBE (11), we include the six energetically highest valence bands, the two energetically lowest s-like conduction bands, and the six energetically lowest p-like conduction bands. Evaluation of the summations over $\mathbf{k}$ space and the band indices for the Hartree-Fock term in Eq. (12) is the most demanding part of the numerical solution of the SBE. With the total of 14 subbands, there are $14^4 = 38\,416$ combinations of band indices for the Coulomb matrix elements. By considering only the Coulomb matrix elements between the six energetically highest valence bands and the two energetically lowest conduction bands, i.e., the electron-hole attraction between the bands that are relevant when exciting resonantly at or near the band gap, this number reduces to $6^2 \times 2^2 = 144$ combinations. We discretize the in-plane $\mathbf{k}$ space using a polar grid with 2880 k points. For the integration of the SBE (11), the fourth-order Runge-Kutta method with a time step of 0.02 fs is used.

The linear absorption coefficient is given by $\alpha_{ij}(\omega) \propto \text{Im}[P_j(\omega)]$ $(i, j = x, y, z)$, where $P_j(\omega)$ is the j component of the Fourier transformed optical polarization $\mathbf{P}(t) = e\sum_{c,v,\mathbf{k}}[\boldsymbol{\xi}_{\mathbf{k}}^{cv} x_{\mathbf{k}}^{cv}(t) + \text{c.c.}]$ with $\boldsymbol{\xi}_{\mathbf{k}}^{cv} = -i\hbar\mathbf{v}_{\mathbf{k}}^{cv}/(\varepsilon_{\mathbf{k}}^{c} - \varepsilon_{\mathbf{k}}^{v})$. The interband coherence $x_{\mathbf{k}}^{cv}(t)$ in the above sum is obtained by solving the SBE describing the linear optical response,

$$\begin{aligned}\frac{d}{dt}x_{\mathbf{k}}^{vc} = &-\frac{i}{\hbar}\left(\varepsilon_{\mathbf{k}}^{c} - \varepsilon_{\mathbf{k}}^{v} - i\hbar/T_2\right)x_{\mathbf{k}}^{vc} - \frac{i}{\hbar}e\mathbf{A}(t)\cdot\mathbf{v}_{\mathbf{k}}^{cv}\\ &+\frac{i}{\hbar}\sum_{c',v',\mathbf{k}'} V_{\mathbf{k},\mathbf{k}'}^{v'cc'v} x_{\mathbf{k}'}^{v'c'},\end{aligned} \tag{18}$$

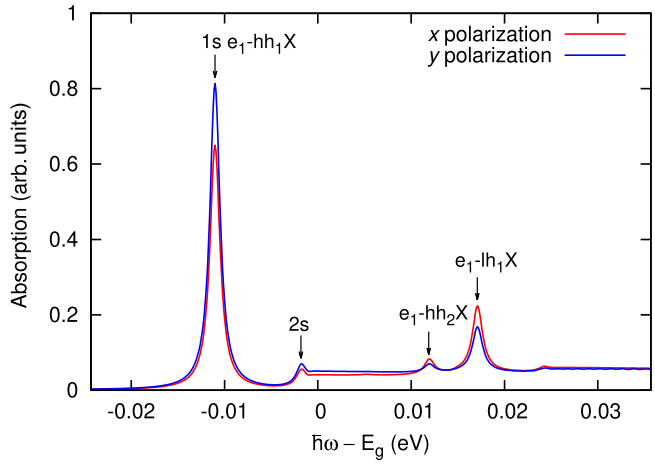

FIG. 1. Linear absorption spectra of a 8 nm (110)-oriented GaAs QW for light polarization in the $x \parallel [001]$ (red line) and $y \parallel [1\bar{1}0]$ (blue line) direction, respectively.

for excitation with an ultrashort pulse that is linearly polarized along the i direction. Here, a dephasing time of $T_2 = 1$ ps was added phenomenologically to describe the decay of the interband polarizations. The linear absorption spectra of the QW are shown in Fig. 1 for different light polarization directions. The spectra exhibit the $1s$ heavy-hole (e_1-hh$_1$) exciton at $\hbar\omega - E_g = -11$ meV, the $2s$ e_1-hh$_1$ exciton at -1.8 meV, the $1s$ e_1-hh$_2$ exciton at 12 meV, and the $1s$ light-hole (e_1-lh$_1$) exciton at 17 meV. Here, $E_g = 1.474$ eV is the band-gap energy of the QW. As has been received in Ref. [33], the difference between the absorption amplitudes for different polarization directions clearly demonstrates the anisotropy of the QW systems which is contained in the electronic band structure and the wave functions.

Figures 2(a)–2(c) show the time dependence of the x components of the ballistic current $\mathbf{j}_{\rm ball}(t)$, the shift current $\mathbf{j}_{\rm shift}(t)$, and the total current $\mathbf{j}(t)$, which are computed using Eqs. (16), (17), and (15), respectively. These currents are generated by a linearly polarized Gaussian-shaped laser pulse with the polarization direction along the y axis. The pulse duration is of $\tau_L = 150$ fs, which corresponds to a spectral width (FWHM) of about 12 meV. The laser pulse has central photon energies $\hbar\omega$ which vary from 20 below to 60 meV above the band gap. With a maximal amplitude of $E_0 = 5 \times 10^3$ V/cm, we are well within the low-excitation regime, i.e., all currents are of second order in the light-matter interaction.

The currents obtained with and without Coulomb interaction are displayed by the solid blue lines and the dashed red lines in Fig. 2, respectively. When the Coulomb interaction is neglected, the ballistic current vanishes; see dashed red lines in Fig. 2(a). With electron-hole attraction, we obtain a strong ballistic current [see solid blue lines in Fig. 2(a)], which exceeds the magnitude of the shift current [Fig. 2(b)] and flows in an opposite direction. Whereas the temporal envelope of the shift current is determined by the incident laser pulse intensity, the ballistic currents last much longer and decay due to dephasing and relaxation processes. For optical excitations close to the band edge, the ballistic current displays temporal oscillations when the spectral width of the pulse covers at least two excitonic resonances. In particular, for a photon energy detuned by $\Delta = -5$ meV below the band gap, the current oscillates with a period of about 490 fs, corresponding to an energy difference of about $h/490$ fs $= 8.4$ meV, which is very close to the separation of the $1s$ and $2s$ excitonic resonances.

To qualitatively explain the oscillations of the ballistic current, we consider a simple two-band semiconductor model which includes the interband coherence $p_k(t) = x_k^{vc}(t)$ and the occupation $n_k(t) = x_k^{cc}(t) = 1 - x_k^{vv}(t)$. Assuming that the pulse simultaneously excites two excitonic states 1 and 2, we express the interband coherence as $p_k(t) = \bar{p}_{1,k}e^{i\omega_1 t} + \bar{p}_{2,k}e^{i\omega_2 t}$, where ω_1 and ω_2 are excitonic resonance frequencies and $\bar{p}_{i,k}$ $(i = 1, 2)$ are slowly time-varying functions. We then separate $\bar{p}_{i,k}$ into a sum of an even and an odd part as a function of k, $\bar{p}_{i,k} = \bar{p}_{i,k}^{\rm even} + \bar{p}_{i,k}^{\rm odd}$. For weak excitation, the occupation is approximately given by $n_k(t) \simeq |p_k(t)|^2$. Since the ballistic current is evaluated by $j_{\rm ball}(t) \propto \sum_k (v_k^{cc} - v_k^{vv}) n_k(t)$, where v_k^{cc}, $v_k^{vv} \propto k$, only the odd component of the occupation with respect to k,

$$n_k^{\rm odd}(t) \simeq 2{\rm Re}\big[\bar{p}_{1,k}^{\rm even*}\bar{p}_{1,k}^{\rm odd} + \bar{p}_{2,k}^{\rm even*}\bar{p}_{2,k}^{\rm odd}\big] + 2{\rm Re}\big[\big(\bar{p}_{1,k}^{\rm even*}\bar{p}_{2,k}^{\rm odd} + \bar{p}_{1,k}^{\rm odd*}\bar{p}_{2,k}^{\rm even}\big)e^{i(\omega_2-\omega_1)t}\big], \quad (19)$$

contributes to the ballistic current. The first and the second terms in Eq. (19) correspond to contributions to the DC and the AC components of the ballistic current, respectively.

Thus the oscillations seen in Fig. 2(a) near $\Delta = -5$ meV originate from the interference between $1s$ and $2s$ e_1-hh$_1$ excitonic wave packets. Similarly, the oscillations near $\Delta =$ 10 and 20 meV are, respectively, linked to e_1-hh$_2$ and e_1-lh$_1$ excitonic beats, which have longer periods due to the smaller binding energies.

The oscillation of the ballistic current is somewhat similar to that of the two-color photocurrent which has been theoretically obtained in semiconductor quantum wires [34]. However, for the case of the two-color photocurrent, the oscillation is due to the interference between the $1s$ and the $2p$ excitonic coherences. Unlike the one-color photocurrent, the two-color photocurrent is induced by optical excitation with two frequencies ω and 2ω and is a third-order nonlinear optical process that does not rely on the material symmetry [34–38].

After generation, the calculated ballistic current decreases as a function of time. This decay is due to the electron-LO-phonon scattering. By fitting with an exponential decay $\propto \exp(-t/\tau)$, we obtain, for a photon energy of $\Delta = 30$ meV, a decay time of $\tau \simeq 340$ fs. If Δ is larger than the energy of the optical phonon $\hbar\omega_{\rm LO}$, the current initially decays more rapidly due to the emission of LO phonons. The decay then slows down at longer times when the electron kinetic energy relaxes to a value below $\hbar\omega_{\rm LO}$ and the LO-phonon emission is suppressed.

The shift current shown in Fig. 2(b) basically follows the intensity of the optical pulse, i.e., it has a Gaussian shape centered at $t \simeq 0$. For above-band-edge excitations, the shift current may also have an oscillatory tail. It was shown that for bulk GaAs, this contribution is caused by coherences between the heavy-hole and light-hole valence bands [24]. In QWs, heavy and light holes are mixed and thus the coherences between valence subbands lead to oscillations with frequencies given by the energy spacing between the

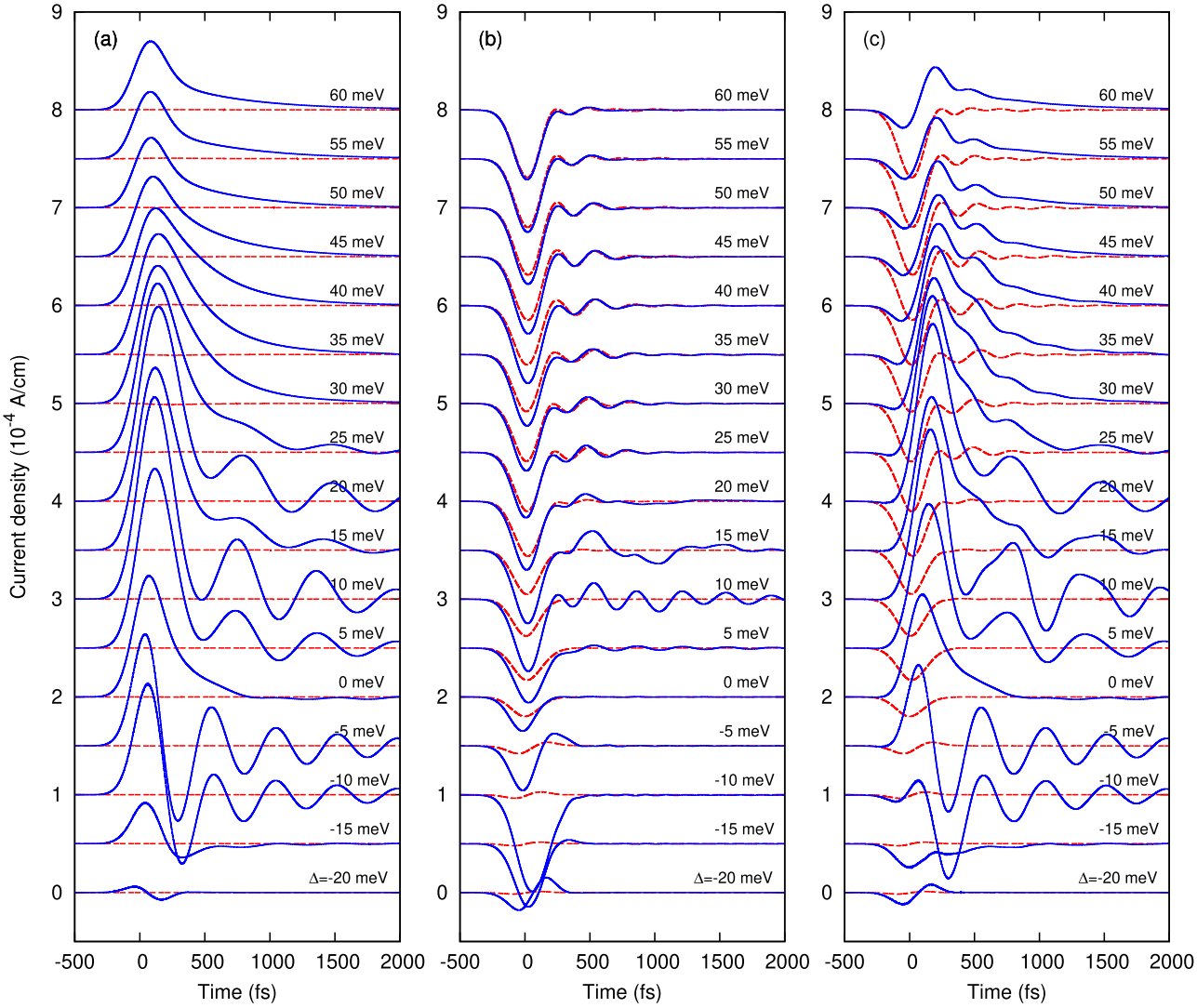

FIG. 2. Time evolution of the x component of (a) the ballistic current, (b) the shift current, and (c) the total current for different photon energy detunings $\Delta = \hbar\omega - E_g$. The currents are calculated with (solid blue lines) and without (dashed red lines) Coulomb interaction. The polarization direction of light is parallel to the y axis ($\theta = 90°$). To improve visibility, the currents for different Δ are shifted vertically.

subbands. In the presence of the electron-hole attraction, because of the Coulomb enhancement of the absorption, the shift current is strongly enhanced for excitations near the band edge. In particular, the shift current shows peaks at $\Delta \simeq -10$ and $\Delta \simeq 10$ meV, which are close to the heavy-hole and light-hole excitonic resonances. Furthermore, we find that the oscillatory tail of the shift current at photon energies in between the heavy-hole and light-hole excitonic resonances ($\Delta \simeq 10$ meV) is of the order of a few picoseconds and is much longer than that at higher photon energies. This can be explained by the longer dephasing time of the coherence between heavy-hole and light-hole excitons in comparison to that of the coherences between uncorrelated holes. Here, we note that the dephasing times are obtained by a microscopic calculation using (14). Our results for the oscillatory components of the shift current as well as the ballistic current are in agreement with experimental observations of the Terahertz emission of GaAs QWs [8,18]. With increasing photon energy, excitonic effects become less important and, therefore, well above the band gap, the results with and without Coulomb interaction approach each other; see Fig. 2(b). It is furthermore noteworthy that for $\Delta = -20$ meV, the excitation is fully nonresonant and in this case the transient appears in Fig. 2(b) which follows the derivative of the intensity of the optical pulse and thus originates from optical rectification.

Comparison of the dashed red and solid blue lines of Fig. 2(c) demonstrates that like the individual contributions, the experimentally measurable total current $\mathbf{j}(t)$, which is the sum of $\mathbf{j}_{\mathrm{ball}}(t)$ and $\mathbf{j}_{\mathrm{shift}}(t)$, is also strongly modified by the electron-hole attraction. Except for the lowest and highest considered excitation frequencies, $\mathbf{j}_{\mathrm{ball}}(t)$ dominates clearly over $\mathbf{j}_{\mathrm{shift}}(t)$ and thus the initial maximum of total current $\mathbf{j}(t)$ is positive. Furthermore, the oscillations originating from quantum beats between the excitonic states are clearly visible in the total current. Therefore, the effects obtained from our numerical analysis should be observable in experiment.

Before examining the dependence of ballistic and shift currents on the orientation of light polarization, we note that (110)-oriented GaAs QWs with the symmetry of the C_{2v} point group have two mirror reflection planes xy and xz. From a

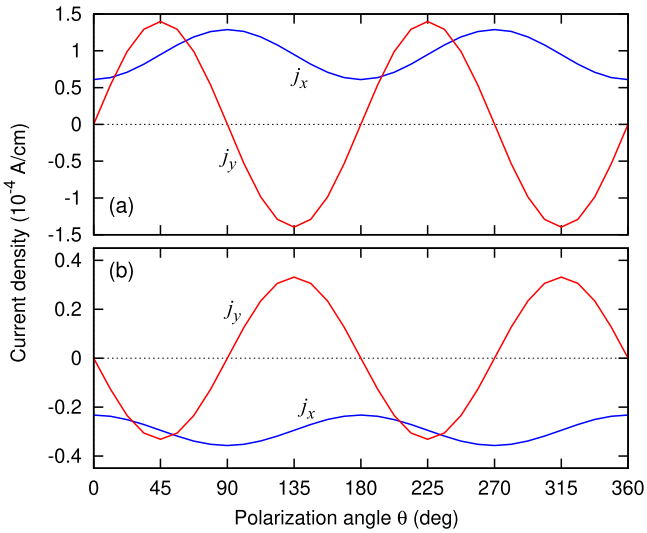

FIG. 3. Components in the x and y directions of the peak values of (a) the ballistic and (b) the shift currents as a function of the light polarization angle θ.

macroscopic symmetry analysis, one obtains, for the second-order current response, the relations

$$j_x = \sigma^{(2)}_{xxx}|E_x|^2+\sigma^{(2)}_{xyy}|E_y|^2, \quad j_y = \sigma^{(2)}_{yxy}E_xE_y^*+\sigma^{(2)}_{yyx}E_yE_x^*. \quad (20)$$

The x and y components of the computed ballistic and shift currents versus the light polarization angle θ, which is defined with respect to the $x \parallel [001]$ direction, are shown in Figs. 3(a) and 3(b), respectively, for the central photon energy of $\hbar\omega = 1.474$ eV, i.e., corresponding to the band gap. The ballistic and shift currents are evaluated at their peak values, i.e., at $t \simeq 100$ fs for the ballistic current and $t \simeq 0$ fs for the shift current. The numerical results of Figs. 3(a) and 3(b) can be formulated as $j_x = A + B\cos 2\theta$ and $j_y = C \sin 2\theta$ and thus perfectly agree with the above symmetry analysis (20). Furthermore, Fig. 3 highlights the stronger magnitude of the ballistic currents and the opposite directions of two currents for all polarization directions.

IV. CONCLUSION

The dynamical generation and decay of photocurrents in GaAs QWs induced by linearly polarized single-frequency laser pulses has been described microscopically. We demonstrate that the electron-hole attraction gives rise to a strong ballistic current, which is absent when the Coulomb interaction is neglected, and also enhances the shift current when exciting near excitonic resonances. The strength of the Coulomb-induced ballistic current is stronger than that of the shift current and their directions are opposite. We have also shown that the coherent dynamics of excitonic wave packets leads to oscillations in the transients of the ballistic current.

These are general effects that should be present in all noncentrosymmetric semiconductors. The existence of ballistic currents solely originating from the asymmetric electron-hole attraction offers novel possibilities for exploring the coherent dynamics of excitons. Using appropriate materials and nanostructures, the excitonic energy differences can be tuned and might be used to generate oscillatory currents with particular frequencies in the Terahertz range on ultrafast timescales.

ACKNOWLEDGMENTS

We would like to thank M. Bieler for several useful discussions. This work is funded by the Vietnam National Foundation for Science and Technology Development (NAFOSTED) under Grant No. 103.01-2017.42 and by the Deutsche Forschungsgemeinschaft (DFG) through Project No. ME 1916/4. We thank the PC^2 (Paderborn Center for Parallel Computing) for providing computing time.

[1] V. I. Belinicher and B. I. Sturman, Sov. Phys. Usp. **23**, 199 (1980).
[2] B. I. Sturman and V. M. Fridkin, *The Photovoltaic and Photorefractive Effects in Noncentrosymmetric Materials* (Gordon and Breach, Philadelphia, 1992).
[3] J. E. Sipe and A. I. Shkrebtii, Phys. Rev. B **61**, 5337 (2000).
[4] V. I. Shelest and M. V. Éntin, Sov. Phys. Semicond. **13**, 1353 (1979).
[5] V. I. Belinicher, E. L. Ivchenko, and B. I. Sturman, Zh. Eksp. Teor. Fiz. **83**, 649 (1982) [Sov. Phys. - JETP **56**, 359 (1982)].
[6] D. Côté, N. Laman, and H. M. van Driel, Appl. Phys. Lett. **80**, 905 (2002).
[7] F. Nastos and J. E. Sipe, Phys. Rev. B **74**, 035201 (2006).
[8] P. C. M. Planken, M. C. Nuss, I. Brener, K. W. Goossen, M. S. C. Luo, S. L. Chuang, and L. Pfeiffer, Phys. Rev. Lett. **69**, 3800 (1992).
[9] J. B. Khurgin, J. Opt. Soc. Am. B **13**, 2129 (1996).
[10] P. Král, J. Phys.: Condens. Matter **12**, 4851 (2000).
[11] S. D. Ganichev, E. L. Ivchenko, S. N. Danilov, J. Eroms, W. Wegscheider, D. Weiss, and W. Prettl, Phys. Rev. Lett. **86**, 4358 (2001).
[12] L. E. Golub, Phys. Rev. B **67**, 235320 (2003).
[13] N. Laman, M. Bieler, and H. M. van Driel, J. Appl. Phys. **98**, 103507 (2005).
[14] M. Bieler, K. Pierz, and U. Siegner, J. Appl. Phys. **100**, 83710 (2006).
[15] M. Bieler, K. Pierz, U. Siegner, and P. Dawson, Phys. Rev. B **76**, 161304(R) (2007).
[16] S. Priyadarshi, A. M. Racu, K. Pierz, U. Siegner, M. Bieler, H. T. Duc, J. Förstner, and T. Meier, Phys. Rev. Lett. **104**, 217401 (2010).
[17] H. T. Duc, J. Förstner, and T. Meier, Phys. Rev. B **82**, 115316 (2010).
[18] S. Priyadarshi, K. Pierz, U. Siegner, P. Dawson, and M. Bieler, Phys. Rev. B **83**, 121307(R) (2011).
[19] S. M. Young and A. M. Rappe, Phys. Rev. Lett. **109**, 116601 (2012).
[20] S. M. Young, F. Zheng, and A. M. Rappe, Phys. Rev. Lett. **110**, 057201 (2013).
[21] J. A. Brehm, S. M. Young, and A. M. Rappe, J. Chem. Phys. **141**, 204704 (2014).
[22] C. Somma, K. Reimann, C. Flytzanis, T. Elsaesser, and M. Woerner, Phys. Rev. Lett. **112**, 146602 (2014).

[23] H. T. Duc, R. Podzimski, S. Priyadarshi, M. Bieler, and T. Meier, Phys. Rev. B **94**, 085305 (2016).
[24] R. Podzimski, H. T. Duc, and T. Meier, Phys. Rev. B **96**, 205201 (2017).
[25] A. Ghalgaoui, K. Reimann, M. Woerner, T. Elsaesser, C. Flytzanis, and K. Biermann, Phys. Rev. Lett. **121**, 266602 (2018).
[26] A. M. Burger, R. Agarwal, A. Aprelev, E. Schruba, A. Gutierrez-Perez, V. M. Fridkin, and J. E. Spanier, Sci Adv. **5**, eaau5588 (2019).
[27] E. O. Göbel, K. Leo, T. C. Damen, J. Shah, S. Schmitt-Rink, W. Schäfer, J. F. Müller, and K. Köhler, Phys. Rev. Lett. **64**, 1801 (1990).
[28] M. Koch, J. Feldmann, G. von Plessen, E. O. Göbel, P. Thomas, and K. Köhler, Phys. Rev. Lett. **69**, 3631 (1992).
[29] J. Feldmann, T. Meier, G. von Plessen, M. Koch, E. O. Göbel, P. Thomas, G. Bacher, C. Hartmann, H. Schweizer, W. Schäfer, and H. Nickel, Phys. Rev. Lett. **70**, 3027 (1993).
[30] R. Winkler, *Spin-orbit Coupling Effects in Two-Dimensional Electron and Hole Systems* (Springer, Berlin, 2003).
[31] G. D. Mahan, *Many-particle Physics*, (Plenum, New York, 1981).
[32] H. Haug and S. W. Koch, *Quantum Theory of the Optical and Electronic Properties of Semiconductors*, 4th ed. (World Scientific, Singapore, 2004).
[33] D. Gershoni, I. Brener, G. A. Baraff, S. N. G. Chu, L. N. Pfeiffer, and K. West, Phys. Rev. B **44**, 1930(R) (1991).
[34] D. H. Marti, M.-A. Dupertuis, and B. Deveaud, Phys. Rev. B **72**, 075357 (2005).
[35] E. Dupont, P. B. Corkum, H. C. Liu, M. Buchanan, and Z. R. Wasilewski, Phys. Rev. Lett. **74**, 3596 (1995).
[36] R. Atanasov, A. Haché, J. L. P. Hughes, H. M. van Driel, and J. E. Sipe, Phys. Rev. Lett. **76**, 1703 (1996).
[37] A. Haché, Y. Kostoulas, R. Atanasov, J. L. P. Hughes, J. E. Sipe, and H. M. van Driel, Phys. Rev. Lett. **78**, 306 (1997).
[38] R. D. R. Bhat and J. E. Sipe, Phys. Rev. B **72**, 075205 (2005).